Science Advances
AAAS

Supplementary Materials for

Changes in supramolecular organization of cyanobacterial thylakoid membrane complexes in response to far-red light photoacclimation

Craig MacGregor-Chatwin, Dennis J. Nürnberg, Philip J. Jackson, Cvetelin Vasilev, Andrew Hitchcock, Ming-Yang Ho, Gaozhong Shen, Christopher J. Gisriel, William H. J. Wood, Moontaha Mahbub, Vera M. Selinger, Matthew P. Johnson, Mark J. Dickman, Alfred William Rutherford, Donald A. Bryant, C. Neil Hunter*

*Corresponding author. Email: c.n.hunter@sheffield.ac.uk

Published 9 February 2022, *Sci. Adv.* **8**, eabj4437 (2022)
DOI: 10.1126/sciadv.abj4437

The PDF file includes:

Other Supplementary Material for this manuscript includes the following:

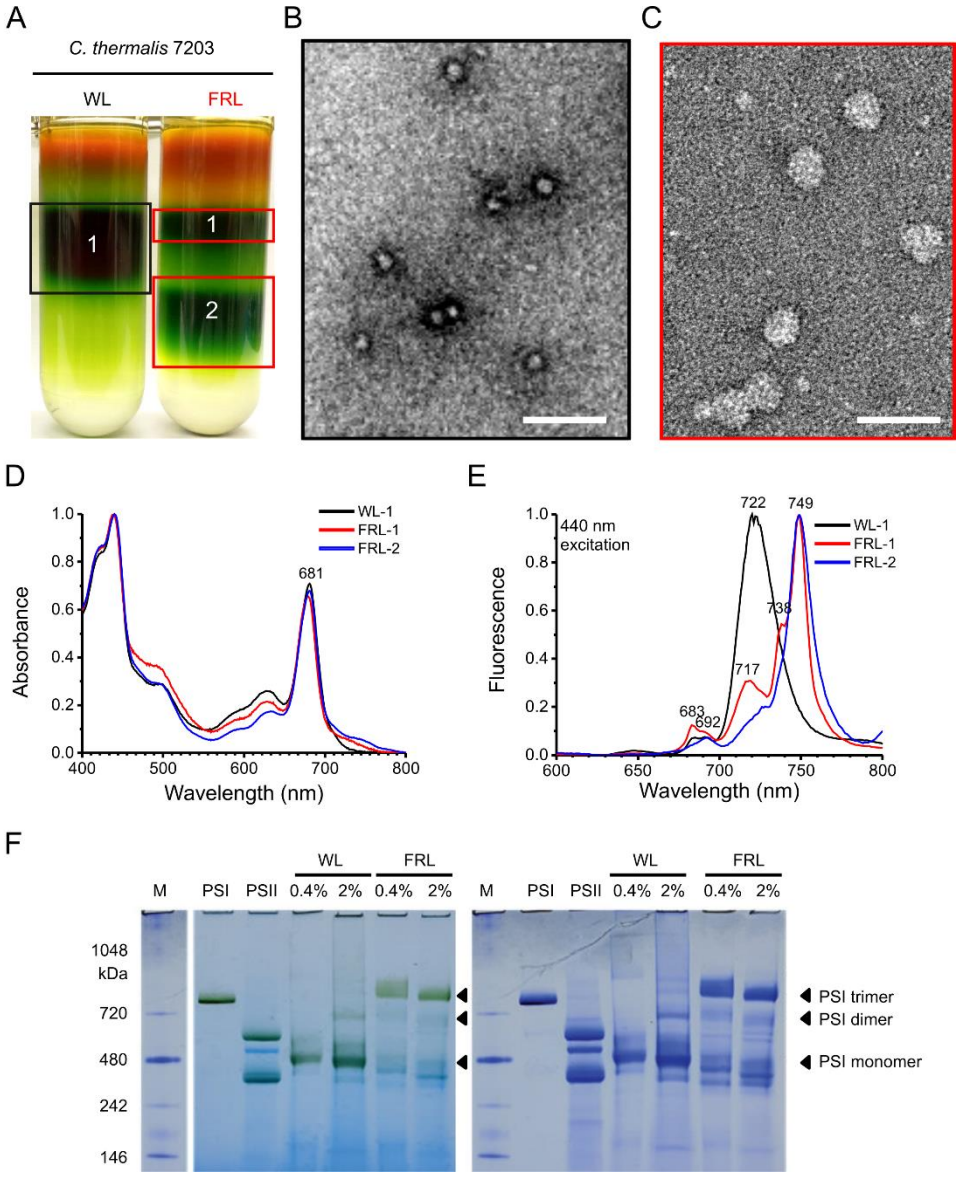

Fig. S1. Characterisation of photosystem complexes solubilised from thylakoid membranes from WL- and FRL-acclimated *C. thermalis* 7203. (**A**) Sucrose density gradients of solubilised membranes from WL (left) and FRL (right) cells showing green bands that correspond to different oligomeric states as described in the main text. (**B**) Negative stain transmission EM of the green band highlighted by the black rectangle "1" in (**A**) showing either monomeric or dimeric complexes. (**C**) Negative stain transmission EM of the band highlighted in the red rectangle "2" in (**A**) showing trimeric PSI complexes purified from FRL membranes. Scale bars in (**B**) and (**C**) are 50 nm. (**D**) Room temperature absorbance spectra of bands from the sucrose gradients in (**A**). (**E**) 77 K fluorescence emission spectra of bands from the sucrose gradients in (**A**). (**F**) BN-PAGE analysis of thylakoid membranes from WL- and FRL-acclimated *C. thermalis* 7203 (left, unstained gel; right, Coomassie-stained gel). Thylakoid membranes were solubilized in 0.4 % and 2 % (w/v) β-DDM as indicated. Isolated photosystems from *T. elongatus* were used for comparison, showing trimeric PSI and monomeric and dimeric PSII with an unknown protein complex in between. NativeMARK Protein Standard (Novex) was used as a molecular weight marker (M). Approximately 1.5 µg Chl was loaded for each condition.

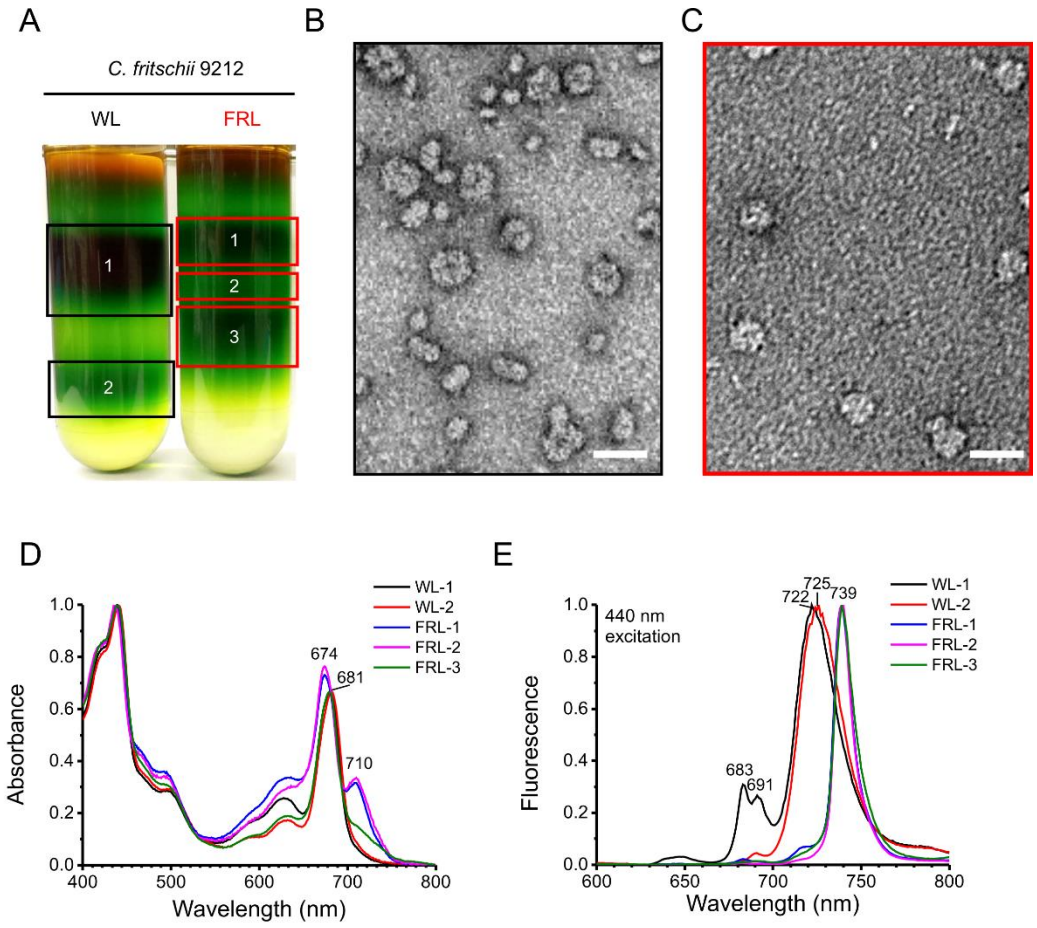

Fig. S2. Characterisation of photosystem complexes solubilised from thylakoid membranes from WL- and FRL-acclimated *C. fritschii* 9212. (**A**) Sucrose density gradients of solubilised membranes from WL (left) and FRL (right) cells showing green bands that correspond to different oligomeric states as described in the main text. (**B**) Negative stain transmission EM of the green band highlighted by the black rectangle "2" in (**A**) showing either dimeric or tetrameric complexes from WL membranes. (**C**) Negative stain transmission EM of the band highlighted in the red rectangle "3" in (**A**) showing trimeric PSI complexes purified from FRL-acclimated membranes. Scale bars in (**B**) and (**C**) are 50 nm. (**D**) Room temperature absorbance spectrum of bands from the sucrose gradients in (**A**). (**E**) 77 K fluorescence emission spectra of bands from the sucrose gradients in (**A**).

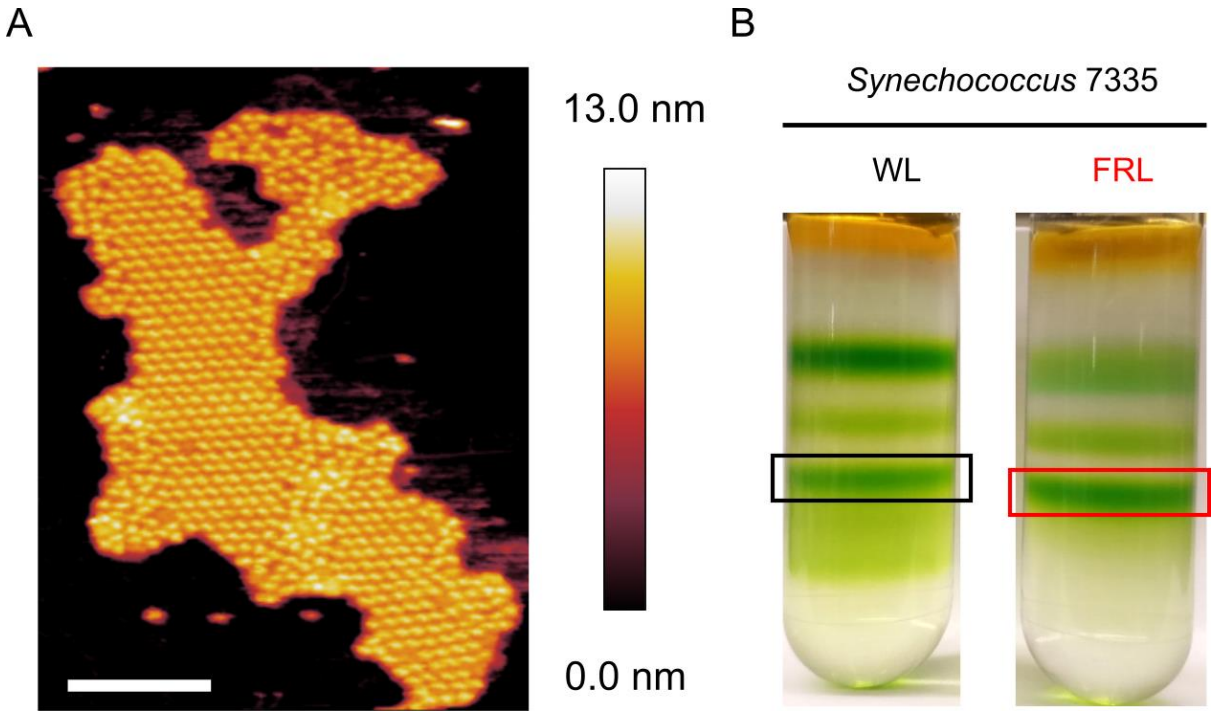

Fig. S3. Characterisation of PSI complexes in WL- and FRL-acclimated membranes from *Synechococcus* 7335. (**A**) AFM of thylakoid membranes from *Synechococcus* 7335 showing large arrays of PSI complexes in either a dimeric or tetrameric configuration with peripheral regions of trimeric PSI complexes in a disordered state, showing that both configurations are present in WL membranes. Scale bar is 100 nm.. (**B**) Sucrose density gradients of solubilised membranes from WL (left) and FRL (right) cells in which green bands can be observed that correspond to different oligomeric states of photosynthetic complexes. The black rectangle highlights the green band that corresponds to trimeric PSI in WL membranes. The red rectangle highlights the major band in the density gradient, which corresponds to PSI trimers, and suggests an increased proportion of trimeric PSI complexes in FRL-acclimated membranes.

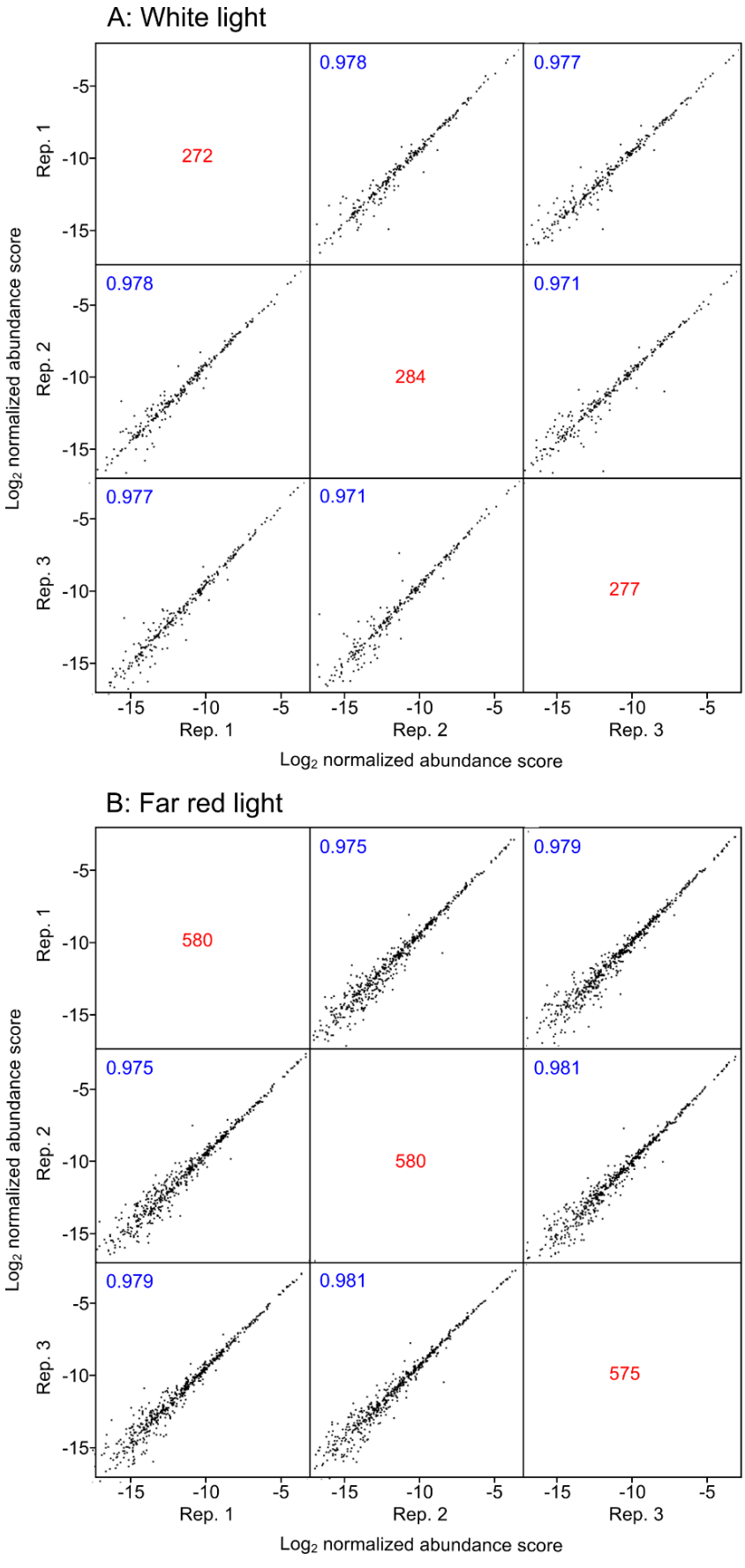
A: White light
0.978
0.977
272
0.978
0.971
284
0.977
0.971
277
Rep. 1
Rep. 2
Rep. 3
-5
-10
-15
Log2 normalized abundance score
B: Far red light
0.975
0.979
580
0.975
0.981
580
0.979
0.981
575
Rep. 1
Rep. 2
Rep. 3
-5
-10
-15
Log2 normalized abundance score

Fig. S4. Correlation matrices for three technical replicate proteomic analyses of thylakoid membranes from *C. thermalis* cells acclimated under (A) WL and (B) FRL. Thylakoid membranes were subjected to quantitative proteomic analysis in triplicate as described in Materials and Methods, with protein abundance scores calculated by the iBAQ method and normalized to the intra-analysis sum of iBAQ abundance scores. The numbers of protein identifications for each replicate are shown in red and the Spearman rank correlation coefficients in blue. A total of 629 proteins were quantified and the data-points are listed in Supplementary Data S1.

A

```
PsaA1      MTISPPEREEKKARVVVDNDPVPTSFELWSKPGHFDRTLSRGPKTTTWIWNLHALAHDFD      60
PsaA2      MTITP--EREQKVRVVVDNDPVPTSPELWAKPGHFDRTLARGPKTTTWIWNLHANAHDFD      58

PsaA1      THTSDLEDISRKIFAAHFGHLAVIFIWLSGMYFHGARFSNYEAWLADPLGVKPSAQVVWS      120
PsaA2      THTSDLEDISRKIFAAHFGHLAVIFIWLSGMYFHGAKFSNFEAWMANPTGVKPSAQVVWS      118

PsaA1      VVGQDILNADVGGGFHGIQITSGFFQIWRGAGITNTFQLYCTAIGGLVMAALMLFAGWFH      180
PsaA2      LVGQDILNADVGGGFHGIQITSGLFQLWRAAGITNTFQLYCTAIGGLVMAAIMLFAGWFH      178

PsaA1      YHKRAPKLEWFQNVESMLNHHLAGLLGLGSLAWAGHQIHVSLPINKLLDAGVAPKDIPLP      240
PsaA2      YHKRAPKLEWFQNWEAMMNHHLAGLLGLGCLGWAGHQIHVALPVNKLLDAGVAIKDIPLP      238

PsaA1      QEFILNSNLMTELYPSFAQGLTPFWTLNWGAYADFLTFKGGLNPVTGGLWLTDQAHHHLA      300
PsaA2      HEFILNTSLMAELYPSFAKGLVPFFTLQWGQYADFLTFKGGLNPVTGGLWLSDTAHHHLA      298

PsaA1      IAVLFIIAGHMYRTNWGIGHSLKEILENHKGPF--------TGDGHRGLFENMTTSWHAQ      352
PsaA2      LAVLFIVAGHFYRTNWGIGHSFKEMLDDAKSPNMLPFLNFIGPVGHEGLDKIFETSWHAN      358

PsaA1      LGTNLAMLGSLTIIVAHHMYAMPPYPYLATDYATQLSIFTHHMWIGAFCIVGGAAHATIF      412
PsaA2      LSIHLVQFGTASLLVAHHMYAMPPYPYLATDYATALSLFTHHVWIAGFCIVGGAAHAAIF      418

PsaA1      MVRDYDPATNMNNVLDRVLRHRDAIISHLNWVCMFLGFHSFGLYIHNDTMQALGRPQDMF      472
PsaA2      MVRDYDPAHHVNNILDRTLRHRDVIISHLAWVCQFLGFHSFAMYCHNDTMRAFGRPQDMF      478

PsaA1      SDTAIQLQPVFAQWVQNLHTLAP----------------------GSTAPNALEPVSY      508
PsaA2      SDTGIQLQPIFAQWIQHIHTAAVGAAQVAQPLGDVFGGVRGIELSGLGTTAPGIGAPVSY      538

PsaA1      AFGGGVLAVGGKVAMMPIALGTADFMIHHIHAFQIHVTVLILLKGFLFARNSRLIPDKAN      568
PsaA2      AWGGGMVAVGGKVAMMPIALGTADFLIHHIHAFTIHVTVLVLFKGVLFARGSRLVPDKAN      598

PsaA1      LGFRFPCDGPGRGGTCQVSGWDHVFLGLFWMFNTISIAVYHFSWKMQSDVWGTVDPDGTI      628
PsaA2      LGFRFPCDGPGRGGTCQVSAWDHVFLGLFWMYNSLSMVVFHFSWKMQSDVWGTVDSDGIV      658

PsaA1      NHITAGNWALSATTINGWLRDFQWAQAAQVIQSYGSALSAYGLLFLGAHFVWAFSLMFLF      688
PsaA2      THLTGGNFATSSITNNGWLRDFLWAQSAQVIQSYNSSLSAYGLMFLAGHFIFGFSLMFLF      718

PsaA1      SGRGYWQELIESIVWAHNKLKVAPTVQPRALSIIQGRAVGVAHYLLGAIVTIWAFFEARI      748
PsaA2      SGRGYWQELIESIVWAHNKLKVAPAIQPRALSIVHGRAVGVAHYLLGGIVTTWAFFLARM      778

PsaA1      LSVG  752
PsaA2      SAIG  782
```

B

```
PsaB1      MATKFPKFSQDLAQDPTTRRIWYGIATAHDFESHDGMTEENLYQKLFATHFGHLAIIFLW      60
PsaB2      MATKFPKFSQDLAQDPTTRRIWYAMATAHDFELHDGMTEENLYQKIFASHFGHLAIIFLW      60

PsaB1      ASSLLFHVAWQGNFEQWIKDPLHVRPIAHAIWDPQFGKAAVDAFTQGGASYPVNIAYSGV      120
PsaB2      ASGVLFHVAWQGNFEQWIKDPLNVRPIAHAIWDAQFGPPAIEAFTRAGATNPVDICYSGV      120

PsaB1      YHWWYTIGMRTNNDLYMGSVFLLLLASLFLFAGWLHLQPKFRPSLSWFKSAEPRLNHHLA      180
PsaB2      YHWWYTIGMRTNNELYVGAIFLLLLAALFLFAGWLHLQPRYRPTLGWFKSAEPRLNHHLA      180

PsaB1      GLFGVSSLAWTGHLVHVAIPESRGQHVGWSNFLTTPPHPDGLQPFFSGNWGAYAANPDTA      240
PsaB2      GLFGVSSLAWAAHLIHVAIPESRGQHVGWDNFLFTPPHPAGLGAFFTGNWSAYAQNPDTA      240

PsaB1      NHVFGTSQGAGTAILTFLGGFHPQTQSLWLTDMAHHHLAIAVLFIVAGHMYRTNFGIGHS      300
PsaB2      QHVFNSSQGAGTAILTFLGGFHPQTQSLWLTDMAHHHVAIAVLFIIAGHMYRTNWGIGHS      300

PsaB1      IKEMLNAKKFFGASTEGQFNLPHQGLYDTINNSLHFQLSLALAALGTITSLVAQHMYAMP      360
PsaB2      IKEMLNSKSFFGAKVEGPFNLPHQGLYDTINNSLHFQLSFALAALGVASSLTAQHMYSMP      360

PsaB1      PYAFIGQDFTTQAALYTHHQYIACALMLGAFAHAAIFWVRDYDPEQNKGNVLDRVLKHKE      420
PsaB2      PYAFIGQDFTTQAALYTHHQYIAGFLMVGAFSHAGIFWIRDYDPEQNKGNVLDRMLRHKE      420

PsaB1      AIISHLSWVSLFLGFHTLGLYVHNDVVVAFGTPEKQILIEPVFAQFIQGAHGKVLYGFDT      480
PsaB2      AIISHLSWVSLFLGFHTLGLYVHNDVEVAFGAAEKQVLIEPVFAQFIQAAHGKALYGFNT      480

PsaB1      LLSNPDSVASTA----GAAWLPNWLDAINNGTNSLFLTIGPGDFLVHHAFALAIHTTVLV      536
PsaB2      LLSNPDSIASTAWPNHANVWLPGWLDAVNNTTNSLFLTIGPGDFYVHHAIALGLHVTTLV      540

PsaB1      LVKGALDARGSKLMPDKKDFGYAFPCDGPGRGGTCDISAWDSFYLAAFWVLNTAGWVTFY      596
PsaB2      LVKGALDARGSKLMPDKKDFGYAFPCDGPGRGGTCDISAWDASYLAVFWMLNTLGWVTFY      600

PsaB1      WHWKHLGIWQGNVAQFNESSTYLMGWLRDYLWLYSAQLINGYNPYGMNNLSVWAWMFLLG      656
PsaB2      WHWKHLAIWEGNIAQFNESSTYLMGWFRDYLWLHSAQLINGYNPYGTNSLAIWSWMFLWG      660

PsaB1      HLIWATGFMFLISWRGYWQELIETLVWAHERTPLANLIRWKDKPVALSIVQARIVGLGHF      716
PsaB2      HLAWAVSFMFLITWRGYWQELIETLVWAHEKTPLS-FGYWRDKPVALSIVQARLVGLTHF      719

PsaB1      AAGYILTYAAFLIASTAGKFG  737
PsaB2      TVGYIATYGAFLIASTAGKFG  740
```

Fig. S5 Alignment of PsaA and PsaB homologs showing the location of shared tryptic peptides. Proteomic analysis most often employs upstream proteolysis with trypsin to generate peptide fragments for nano-flow liquid chromatography coupled on-line to mass spectrometry. Protein homologs with a significant degree of sequence identity may contain shared tryptic peptides. This situation is exemplified by isoforms of the photosystem I subunits (**A**) Chro_5026/1019 (PsaA1/A2) and (**B**) Chro_5027/1018 (PsaB1/B2), with shared peptides highlighted in colored rectangles. For quantification of differential expression by iBAQ, which utilizes the sum of all peptide ion intensities attributable to each protein, peptides with ion intensities contributed by more than one isoform may introduce inaccuracy. For relative quantification of photosystem subunit isoforms, we instead used the Top-N method in which the three most intense and unique tryptic peptide ion intensities mapping to a protein were summed to generate the abundance score.

Fig. S6. Sequence alignments of PsaL from *Synechocystis* 6803 with FaRLiP encoded PsaL2 subunits from *C. fritschii* 9212, *C. thermalis* 7203 and *Synechococcus* 7335. The sequences for the FaRLiP encoded PsaL2 subunits that are incorporated into trimeric PSI complexes have been aligned with the PsaL subunit from *Synechocystis* 6803, which also forms trimeric complexes. The colored boxes show the four conserved amino acid residues that have been identified as important for trimer formation.

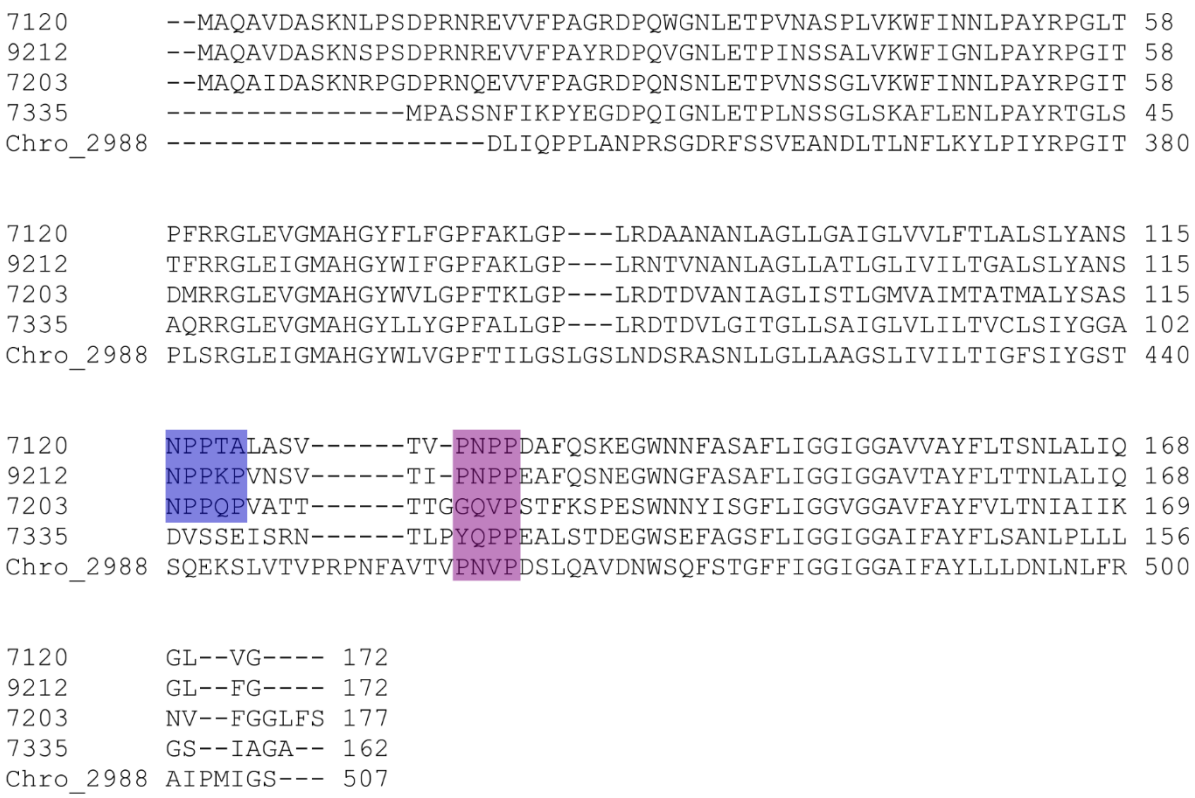

Fig. S7. Sequence alignments of PsaL from Anabaena 7120 with non-FaRLiP encoded PsaL1 subunits from *C. fritschii* 9212, *C. thermalis* 7203, *Synechococcus* 7335 and the PsaL domain of the Chro_2988 protein from *C. thermalis* 7203. The sequences for the PsaL1 subunits preferentially expressed under WL growth conditions in addition to the PsaL domain of the Chro_2988 protein have been aligned to show the presence or absence of 2 multiproline motifs (highlighted in blue and purple), commonly found in PsaL subunits that do not form trimeric complexes.

```
9212-WL  ----------MAASFLPSIFVPLTGLVFPFVAMAFLFVYIEREDLV----------------------- 36
7203-WL  ---------MFSASFLPSILVPLTVLVFPSVAMALLFLYIEREDPSGI--------------------- 39
7335-WL  ----------MSASFLPTILVPTVGLVFPAIAMAALFLYIERGQATTGGESAPWGQVSEDSQ---TDVV- 56
9212-FRL MVDMTQLTGDYAASWLPWIMIPLIFYILPFPVFAILFLWIQKEDSEQIQETDSNLAKVGELEAPKP---- 66
7203-FRL MVDMTQLTGSYAASWLPWIMIPLIFYILPFPVFALIFIWIEKEAGTADEEV------------------- 51
7335-FRL MVDATQLEGAYAAAWLPWIMIPMITYILPFPIFAIAFLWIEREGGEGGLDIDVMGSNAMSNEAMGRDISS 70
```

Fig. S8. Sequence alignments of FaRLiP encoded and non-FaRLiP encoded PsaI subunits from *C. fritschii* 9212, *C. thermalis* 7203 and *Synechococcus* 7335. The sequences of both versions of the PsaI subunit from all three organisms investigated in this study were aligned to show the presence of a motif at the N-terminus of the PsaI2 proteins preferentially expressed under FRL growth conditions (orange) is absent in the PsaI1 subunits that are expressed under WL.

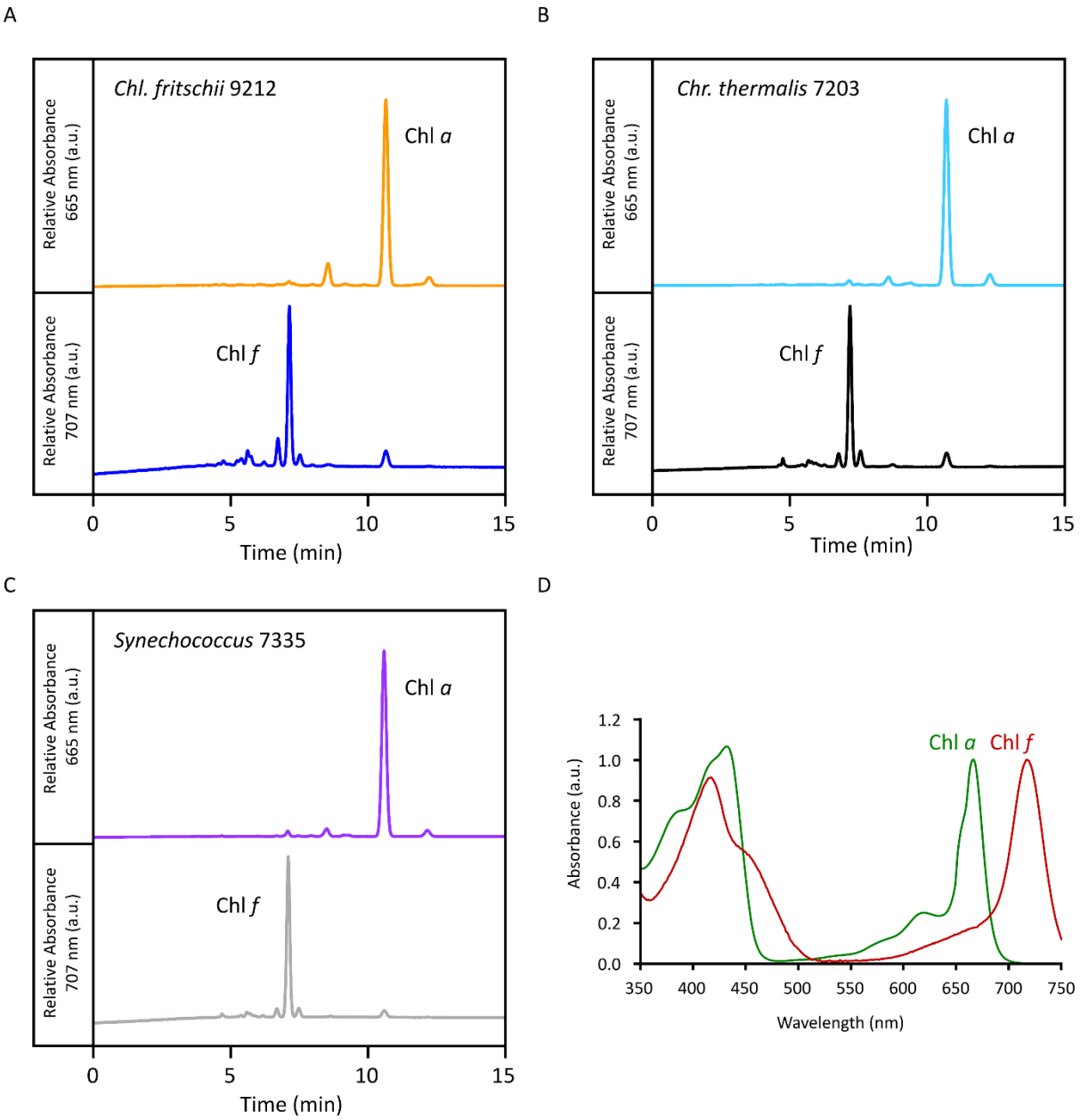

Fig. S9. Analysis of pigments from cyanobacteria grown under FRL conditions. Pigments extracted from FRL-acclimated membranes from (**A**) *C. fritschii* 9212, (**B**) *C. thermalis* 7203 and (**C**) *Synechococcus* 7335 were separated by HPLC. Absorbance was monitored at 665 nm (top panels) to show the presence of Chl *a* and 707 nm (bottom panels) to show the presence of Chl *f*. (D) The identity of the pigments were confirmed by their characteristic absorption spectra. HPLC traces (panels **A**-**C**) were normalised to Chl *a* and Chl *f* peaks and absorption spectra (panel **D**) were normalised to the Qy transition peak. In **A**-**C** 0 min corresponds to the start of isocratic elution in 100 % methanol.

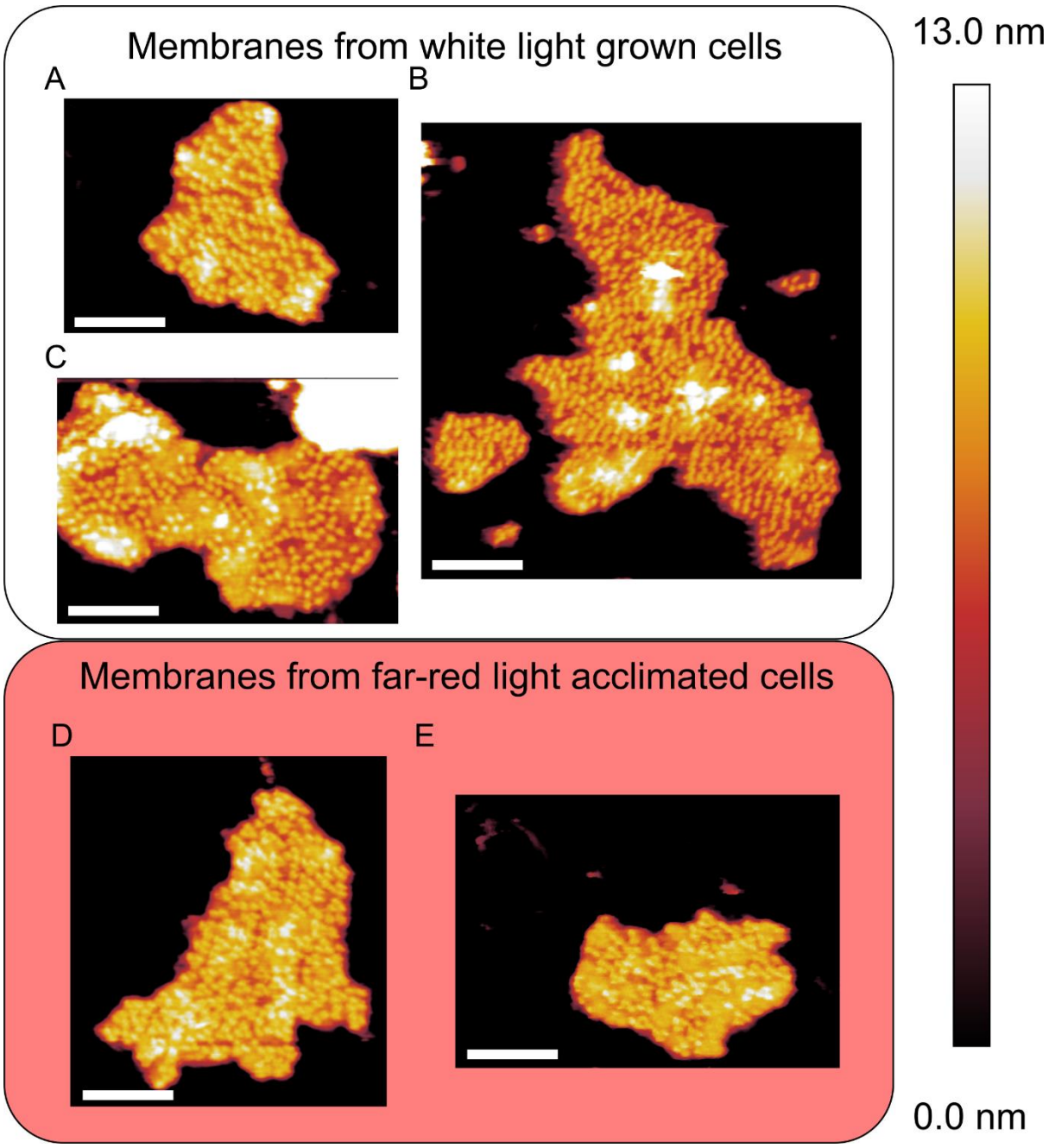

Fig. S10. Gallery of AFM images of thylakoid membranes from WL- and FRL-acclimated *C. thermalis* 7203. (**A**-**C**) AFM topographs of thylakoid membranes from *C. thermalis* 7203 grown under WL showing large areas of membrane containing PSI complexes in either a dimeric or tetrameric configuration. (**D**-**E**) Thylakoid membranes from FRL acclimated *C. thermalis* 7203 cells imaged by AFM showing PSI complexes in a trimeric configuration. Scale bars are 100 nm.

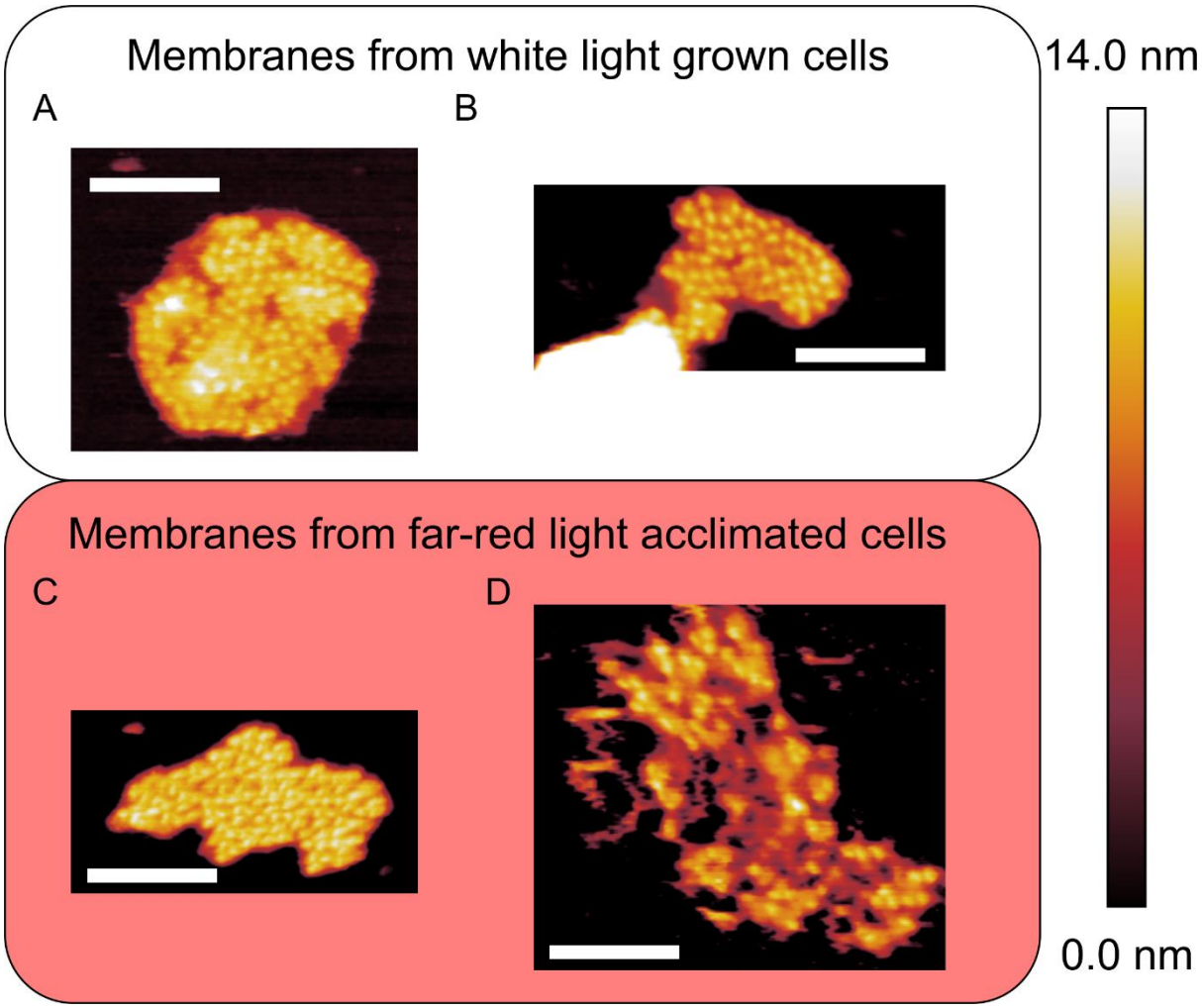

Fig. S11. Gallery of AFM images of thylakoid membranes from WL- and FRL-acclimated *C. fritschii* 9212. (**A** and **B**) Thylakoid membranes from *C. fritschii* 9212 grown under WL imaged by AFM showing PSI complexes in either a dimeric or tetrameric configuration. (**C**-**D**) AFM imaging of thylakoid membranes from FRL acclimated *C. fritschii* 9212 cells showing PSI complexes in a trimeric configuration. Scale bars are 100 nm.

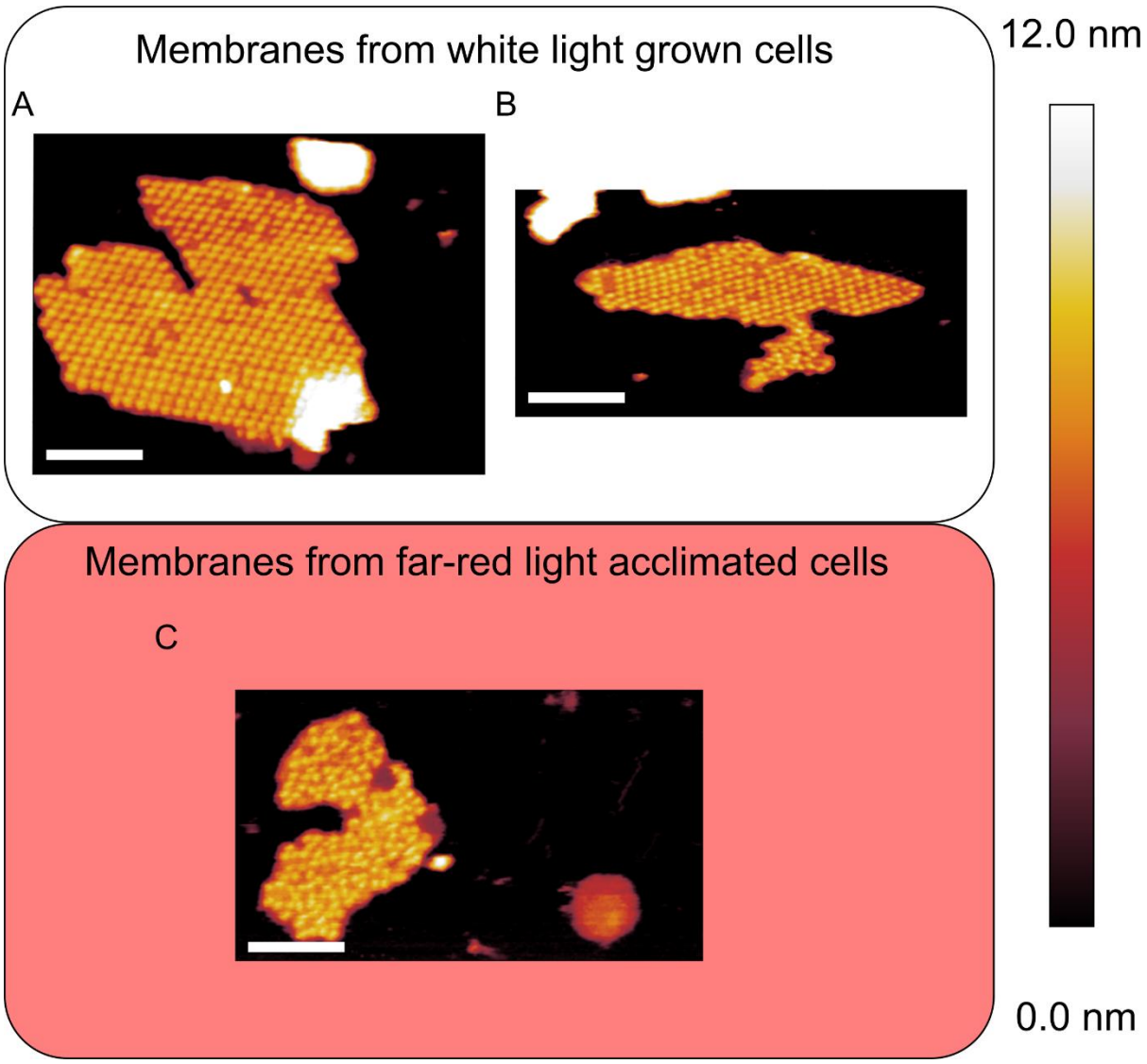

Fig. S12. Gallery of AFM images of thylakoid membranes from WL- and FRL-acclimated *Synechococcus* 7335. (**A** and **B**) *Synechococcus* 7335 thylakoid membranes isolated from cells grown under WL imaged by AFM showing PSI complexes in either a dimeric or tetrameric configuration forming pseudo-crystalline arrays. (**C**) Thylakoid membrane patch from FRL acclimated *Synechococcus* 7335 cells imaged by AFM showing PSI complexes in a trimeric configuration in a disordered array. Scale bars are 100 nm.

Data S1. (separate file)

This data set is from *Chroococcidiopsis thermalis* PCC7203 cells were acclimated under white and far-red light illumination. Proteins were extracted from thylakoid membranes and digested with endoproteinase Lys-C and trypsin. The resultant peptide fragments were analysed by nanoLC-MS/MS as three technical repeats (Rep 1, 2, 3) and the mass spectra subjected to database searching by MaxQuant as described in Materials and Methods.

Protein abundance scores were derived by the iBAQ (intensity-based absolute quantification) method, as implemented by MaxQuant. These values were normalized using Perseus to the intra-analysis sum of iBAQ scores to compensate for random variability arising from sample loading and MS full-scan/product ion scan data-dependent acquisition patterns. The normalized abundance scores were then transformed to log(2). Missing values resulting from the non-detection of proteins in some analyses were replaced by imputation of random values (shown in blue) derived from a normal distribution and weighted to simulate expected low abundance scores, as implemented in Perseus using the default parameters.

Statistical analysis in Perseus was by a modified t-test to provide the significance threshold at $p < 0.05$. The -log(10) p-values and differences (FRL - WL iBAQ score averages) provide the data-points for the volcano plots in Fig. 4A, C (main article).

Data S2. (separate file)

This Data Set is derived from the same MaxQuant output as Data S1 and is confined to the photosystem subunits that were identified and quantified in both white and far-red light thylakoid protein extracts.

Abundance scores were derived by the Top-N method using tryptic peptide ion intensity values calculated by MaxQuant. These values were normalized using Perseus to the intra-analysis sum of peptide ion intensities to compensate for the random variability arising as described above. Each protein abundance score was determined by summing the normalized intensity values for the 1, 2 or 3 most intense peptide ions, depending on the number of peptides identified.

After transformation of the summed intensity values to log(2), statistical analysis was carried out as described above with the -log(10) p-values and differences (FRL - WL Top-N score averages) used to provide the data-points for the volcano plot in Fig. 4B (main article).